Simple way of finding Ba to Si deposition rate ratios for high photoresponsivity in $BaSi_2$ films by Raman spectroscopy

Yudai Yamashita, Yuuki Takahara, Takuma Sato, Kaoru Toko, Akira Uedono, and Takashi Suemasu

Institute of Applied Physics, University of Tsukuba, Tsukuba, Ibaraki 305-8573, Japan

Since the photoresponsivity of $BaSi_2$ is sensitive to a Ba-to-Si deposition rate ratio (R_{Ba}/R_{Si}), there is a need to determine the optimum value of R_{Ba}/R_{Si}. We grew 0.5 μm-thick $BaSi_2$ films with R_{Ba}/R_{Si} varied from 1.1–3.6 at 580 °C and 0.4–4.7 and 650 °C. The photoresponsivity reached a maximum at R_{Ba}/R_{Si} = 2.2 and 1.2, respectively. Raman spectroscopy revealed that the crystalline quality of $BaSi_2$ became better with decreasing R_{Ba}/R_{Si}. However, as R_{Ba}/R_{Si} decreased further beyond these values, excess Si precipitated, showing that the optimum value of R_{Ba}/R_{Si} should be as small as possible without causing Si precipitates to form.

* Corresponding author at:
Institute of Applied Physics, Faculty of Pure and Applied Sciences, University of Tsukuba, Tsukuba, Ibaraki 305-8573, Japan
Electronic mail: suemasu@bk.tsukuba.ac.jp

We have focused on semiconducting barium disilicide ($BaSi_2$) as a new candidate for solar cell applications,[1] because it possesses attractive properties such as a suitable bandgap for solar cells (~1.3 eV), a high optical absorption coefficient $\alpha = 3 \times 10^4$ cm^{-3} at 1.5 eV (more than 40 times as large as that of crystalline Si),[2-5] a large minority-carrier diffusion length $L \approx 10$ μm,[6] and bipolar doping properties.[7-10] We have achieved energy conversion efficiencies η approaching 10% in p-$BaSi_2$/n-Si heterojunction solar cells,[11-13] which are among the highest performances ever reported for solar cells based on semiconducting silicides. Our next target is $BaSi_2$-pn homojunction solar cells, for which η is expected to exceed 25% according to calculations.[14] Recently, we have reported the operation of homojunction solar cells.[15,16] To achieve solar cells having a high-η requires the formation of high-quality $BaSi_2$ light absorbing materials with a low defect density. In our previous work,[17] we reported that undoped $BaSi_2$ shows n-type conductivity, and the carrier type, carrier concentration, and photoresponsivity of $BaSi_2$ change markedly depending on the Ba-to-Si deposition rate ratio (R_{Ba}/R_{Si}); the photoresponsivity reaches a maximum, and the carrier concentration reaches a minimum at $R_{Ba}/R_{Si} = 2.2$ when $BaSi_2$ films were grown at 580 °C by molecular beam epitaxy (MBE). However, deep level transient spectroscopy (DLTS) studies have revealed that such $BaSi_2$ films still contain defects.[18] First-principles calculations based on VASP code show that Si vacancies (V_{Si}) are most likely to occur in $BaSi_2$,[10] and that these vacancies give rise to localized states within bandgaps. DLTS measurement suggests the presence of point defects rather than extended defects.[18] Therefore, we consider that the defect levels detected by DLTS are caused by V_{Si} and related defects. However, there have been no reports to date in which vacancy-type defects like V_{Si} are directly detected. In this work, we first investigated the dependence of R_{Ba}/R_{Si} on the concentration and/or size of vacancy-type defects using positron annihilation spectroscopy. Positron annihilation spectroscopy is a nondestructive technique suitable for detecting vacancy-type defects in semiconductors and obtaining information on the structure of defects.[19,20] We

next increased the substrate temperature (T_S) during epitaxial growth of $BaSi_2$. This is to compensate for defects by promoting the diffusion of Si atoms from the Si substrate into the grown layers and enhancing the migration of deposited Si and Ba atoms.

We used an MBE system equipped with an electron-beam evaporation source for 10N-Si and standard Knudsen cells for 3N-Ba. We used floating zone (FZ) n-Si(111) substrate (resistivity ρ > 10000 Ωcm) for positron annihilation spectroscopy and Czochralski(Cz) n-Si(111) substrate (ρ < 0.01 Ωcm) for photoresponsivity measurements to ensure that the contribution of photogenerated carriers in the Si substrate to the photoresponsivity was negligibly small. We grew 0.5 μm-thick $BaSi_2$ epitaxial layers by MBE at T_S = 580 or 650 °C. Details of the growth procedure of $BaSi_2$ films were reported previously.[17,23] During the MBE growth, R_{Si} was fixed to be 0.9 nm/min and R_{Ba} was varied from 0.9 to 3.2 nm/min, giving a variation of R_{Ba}/R_{Si} from 1.1 to 3.6. In this study, we also conducted MBE at 650 °C, which is 70 °C higher than the temperature used in our previous experiments. We expect that higher T_S promotes the diffusion of Si atoms from the Si substrate. The R_{Ba}/R_{Si} ratio was varied from 0.4 to 4.7. We then formed a 3-nm-thick a-Si capping layer in situ at 180 °C, which acted as a surface passivation layer.[21] Finally, indium-tin oxide (ITO) electrodes with a diameter of 1-mm and a thickness of 80 nm were sputtered onto the surface, and Al electrodes were formed on the entire back surface.

Reflection high-energy electron diffraction (RHEED) and x-ray diffraction (XRD; Rigaku Smart Lab) analyses have been used to characterize the crystalline quality of the grown layers. Epitaxial growth of *a*-axis oriented $BaSi_2$ was confirmed from the θ–2θ XRD patterns. The full width at half maximum (FWHM) of the $BaSi_2$ 600 peak was measured from the ω-scan rocking curve to evaluate the crystal orientation of $BaSi_2$ films. Photoresponsivity was evaluated at room temperature (RT) with the use of a lock-in technique with a xenon lamp and a 25-cm-focal-length single monochromator (Bunko Keiki SM-1700A and RU-60N). Raman

spectra were measured with a laser Raman spectrometer (JASCO, NRS-5100) based on a frequency doubled Nd:YAG laser (532 nm) at RT. Doppler broadening-positron annihilation spectroscopy was used for defect characterization, and the *S* parameter was evaluated. Details of this spectroscopy have been reported in ref. 22. In general, the characteristic value of *S* expected for the annihilation of positrons due to their trapping by vacancy-type defects is larger than that for positrons annihilated from the free-state. Through this method, vacancy-type defects of various semiconductors (i.e., GaN, $AlON_x$, CIGS) have been investigated.[22-26]

Figure 1(a) shows the *S* parameters of $BaSi_2$ films grown at T_S = 580 °C with various R_{Ba}/R_{Si}. We found that the optical properties changed markedly as R_{Ba}/R_{Si} values were varied, and the maximum photoresponsivity was achieved at R_{Ba}/R_{Si} = 2.2 for samples grown at T_S = 580 °C, as shown in Fig. 1(a).[17] Moreover, the carrier concentration reached a minimum at R_{Ba}/R_{Si} = 2.2 [Fig. 1(b)].[17] Figure 1(b) shows the dependence of the *S* parameter on R_{Ba}/R_{Si}. The *S* parameter reached a minimum at approximately R_{Ba}/R_{Si} = 2.2, and increased when R_{Ba}/R_{Si} decreased or increased from this value. The present results suggest that vacancy-type defects which trap positrons are increased when the value of R_{Ba}/R_{Si} departs from 2.2, and they yield electrons. To decrease the vacancy-type defects in $BaSi_2$ films, we next increased T_S during MBE, and used photoresponsivity as a measure of their optical properties.

Thus far, we have set the growth temperature during MBE at T_S = 580 °C, prioritizing the crystal orientation of $BaSi_2$ in the surface normal direction.[27] In this experiment, we increased T_S by 70 °C to 650 °C. Figure 2(a) shows the θ–2θ XRD and RHEED patterns after MBE for $BaSi_2$ films formed with different values of R_{Ba}/R_{Si}. As shown in Fig. 2(a), sharp streaky RHEED patterns and intense *a*-axis-oriented diffraction peaks in the XRD patterns were observed at R_{Ba}/R_{Si} =2.3–4.7, namely, for samples under a Ba-rich condition. Conversely, as R_{Ba}/R_{Si} decreased, the intensity of *a*-axis-oriented diffraction peaks decreased, and the RHEED streak patterns became diffuse. A halo pattern appeared at R_{Ba}/R_{Si} = 0.4 and 0.9, indicating that

$BaSi_2$ was not formed. Figure 2(b) shows the R_{Ba}/R_{Si} dependence of the FWHM values obtained from the ω-scan x-ray rocking curve using a $BaSi_2$ 600 diffraction peak. The FWHM reached a minimum at $R_{Ba}/R_{Si} = 3.7$ (3) for the 650 (580) °C samples. Smaller FWHM means higher *a*-axis-orientation of $BaSi_2$ films. The optimum R_{Ba}/R_{Si} shifted to a Ba-rich side for growth at an elevated temperature, wherein diffusion of Si atoms from the Si substrate was promoted compared with growth at T_S = 580 °C. This result indicates that the crystal orientation was determined by the Ba/Si atomic ratio. Conversely, the FWHM increased with decreasing R_{Ba}/R_{Si}, indicating that the *a*-axis orientation deteriorated for samples grown under Si-rich conditions. We note that the optimum R_{Ba}/R_{Si} determined from the viewpoint of crystal orientation was different from that determined from the photoresponsivity (i.e., $R_{Ba}/R_{Si} = 3$ and 2.2, respectively, for the 580 °C samples).

Photoresponse spectra of the samples grown at T_S = 650 °C are shown in Fig. 3. A bias voltage $V_{bias} = -0.5$ V was applied to the front-surface ITO electrode with respect to the back-surface Al electrode to extract the photogenerated holes in the $BaSi_2$ film to the ITO electrode. The photoresponsivity reached a maximum of approximately 1.2 A/W at 790 nm at R_{Ba}/R_{Si} = 1.2. This photoresponsivity is approximately 3 times as high as that reported previously for a sample at T_S = 580 °C, denoted by a broken line. This improvement is interpreted to originate from the decrease of vacancy-type defects in the $BaSi_2$ films. We note that for the samples grown at 650 °C the optimum R_{Ba}/R_{Si} shifted to the Si-rich side compared with those grown at 580 °C (R_{Ba}/R_{Si}=2.2), as shown in Fig. 1. Hence, the density of defects unexpectedly decreased at R_{Ba}/R_{Si} = 1.2. As shown in Fig. 2(b), the optimum value of R_{Ba}/R_{Si} shifted to a Ba-rich side from the viewpoint of *a*-axis orientation, in comparing the 580 and 650 °C samples. To find how to determine the optimum R_{Ba}/R_{Si} for photoresponsivity, we performed Raman spectroscopy measurements. Figures 4(a) and 4(b) show the Raman spectra of the 580 and 650 °C samples, respectively, in the range between 200 and 700 cm^{-1} at RT. In all of the samples,

we observed five distinct peaks assigned to the internal vibrations of Si tetrahedra[28-31] with T_h symmetry in the lattice of $BaSi_2$.[32] Here, focusing on the Si-rich side, the transverse optical phonon line of Si (Si_{TO}) was observed at $R_{Ba}/R_{Si} \leq 1.5$ for the 580 °C samples, wherein the photoresponsivity reached a maximum at $R_{Ba}/R_{Si} = 2.2$, i.e., slightly higher than 1.5. The absorption coefficient of $BaSi_2$ at a wavelength of the excited laser light (532 nm) is $\alpha = 3 \times 10^5$ cm^{-1},[2] hence, the penetration depth of the laser light was limited to approximately $1/\alpha \times 3 \approx 0.1$ μm. This value is much smaller than the $BaSi_2$ layer thickness. Thus, the Si_{TO} signal was considered to originate from Si precipitated in the $BaSi_2$ films. For the samples grown at 650 °C, the Si_{TO} line appeared to be more pronounced at $R_{Ba}/R_{Si} \leq 0.9$, and the photoresponsivity was highest at $R_{Ba}/R_{Si} = 1.2$, as shown in Fig. 1. This value was also a little greater than 0.9. The Raman peak from V_{Si} should appear at approximately 480 cm^{-1} according to first-principle calculations.[31] However, this peak wavenumber of V_{Si} is close to the most intense peak of the A_g mode in $BaSi_2$. Therefore, we examined the FWHM value of the peak intensity of the A_g mode to confirm the presence of any contribution from V_{Si}. Figure 4(c) shows the R_{Ba}/R_{Si} dependences of the peak intensity of Si_{TO} and the FWHM values of the peak intensity of the A_g mode. Regardless of T_S, the FWMH of A_g mode decreased with decreasing R_{Ba}/R_{Si}, when grown under Si-rich conditions, meaning that the crystalline quality of $BaSi_2$ films became improved as the R_{Ba}/R_{Si} decreased. Conversely, the peak intensity of Si_{TO} increased sharply when the R_{Ba}/R_{Si} decreased from $R_{Ba}/R_{Si} = 2.2$ and 1.2 at $T_S = 580$ and 650 °C, respectively, at the Si-rich side because of an excess of Si atoms. These R_{Ba}/R_{Si} values are the same as those for highest photoresponsivity. On the basis of these experimental results, the R_{Ba}/R_{Si} ratio should be as small as possible, regardless of T_S, while avoiding formation of Si precipitates. We interpret these results as follows. By growing the $BaSi_2$ films under Si-rich conditions and thereby using small values of R_{Ba}/R_{Si}, vacancy-type defects including V_{Si} might decrease, resulting in a higher photoresponsivity. However, further reductions of R_{Ba}/R_{Si} cause precipitation of crystalline Si

particles in the grown films, giving rise to defects, which thus degrade the photoresponsivity. Raman spectroscopy is an effective means of determining the optimum R_{Ba}/R_{Si} from the viewpoint of optimizing photoresponsivity.

In summary, we fabricated 0.5 μm-thick $BaSi_2$ films at 580 °C by MBE, and investigated the dependence of R_{Ba}/R_{Si} on the *S* parameter with the use of positron annihilation spectroscopy. The *S* parameter showed the same tendency against R_{Ba}/R_{Si} as that of the electron concentration. Thus, we confirmed that vacancy-type defects yield electrons in $BaSi_2$. To reduce such defects, we increased T_S during MBE growth from 580 to 650 °C. The FWHM of the $BaSi_2$ 600 XRD peak reached a minimum at $R_{Ba}/R_{Si} = 4$, and increased sharply for samples growth under Si-rich conditions. Conversely, the photoresponsivity reached a maximum of 1.2 A/W at 790 nm when $V_{bias} = -0.5$ V for a sample grown with $R_{Ba}/R_{Si} = 1.2$. This value is approximately 3 times as high as that previously reported for samples grown at 580 °C. The FWHM of the A_g mode peak, reflecting the density of V_{Si}, decreased for samples grown under Si-rich conditions, whereas the intensity of the Si_{TO} peak increased sharply at $R_{Ba}/R_{Si} \leq 1.5$ and 0.9 for samples grown at 580 and 650 °C, respectively. The photoresponsivity was the highest when R_{Ba}/R_{Si} was a little larger than the point at which the Si_{TO} peak increased. We therefore conclude that we should choose R_{Ba}/R_{Si} to be as small as possible to the extent that the precipitation of c-Si is avoided.

ACKNOWLEDGEMENTS

This work was financially supported by JSPS KAKENHI Grant Numbers 17K18865 and 18H03767 and JST MIRAI.

Reference

[1]T. Suemasu and N. Usami, J. Phys. D **50**, 023001 (2017).

[2]K. Toh, T. Saito, and T. Suemasu, Jpn. J. Appl. Phys. **50**, 068001 (2011).

[3]D. B. Migas, V. L. Shaposhnikov, and V. E. Borisenko, Phys. Status Solidi B **244**, 2611 (2007).

[4]M. Kumar, N. Umezawa, and M. Imai, J. Appl. Phys. **115**, 203718 (2014).

[5]M. Kumar, N. Umezawa, and M. Imai, Appl. Phys. Express **7**, 071203 (2014).

[6]M. Baba, K. Toh, K. Toko, N. Saito, N. Yoshizawa, K. Jiptner, T. Sakiguchi, K. O. Hara, N. Usami, and T. Suemasu, J. Cryst. Growth **348**, 75 (2012).

[7]M. A. Khan, K. O. Hara, W. Du, M. Baba, K. Nakamura, M. Suzuno, K. Toko, N. Usami, and T. Suemasu, Appl. Phys. Lett. **102**, 112107 (2013).

[8]M. A. Khan, K. Nakamura, W. Du, K. Toko, N. Usami, and T. Suemasu, Appl. Phys. Lett. **104**, 252104 (2014).

[9]M. Kobayashi, Y. Matsumoto, Y. Ichikawa, D. Tsukada, and T. Suemasu, Appl. Phys. Express **1**, 051403 (2008).

[10]M. Kumar, N. Umezawa, W. Zhou, and M. Imai, J. Mater. Chem. A **5**, 25293 (2017).

[11]S. Yachi, R. Takabe, K. Toko, and T. Suemasu, Appl. Phys. Lett. **109**, 072103 (2016).

[12]D. Tsukahara, S. Yachi, H. Takeuchi, R. Takabe, W. Du, M. Baba, Y. Li, K. Toko, N. Usami, and T. Suemasu, Appl. Phys. Lett. **108**, 152101 (2016).

[13]T. Deng, T. Sato, Z. Xu, R. Takabe, S. Yachi, Y. Yamashita, K. Toko, and T. Suemasu, Appl. Phys. Express **11**, 6 (2018).

[14]T. Suemasu, Jpn. J. Appl. Phys. **54**, 07JA01 (2015).

[15]K. Kodama, R. Takabe, Tianguo Deng, Kaoru Toko, and Takashi Suemasu, Jpn. J. Appl. Phys. **57**, 050310 (2018).

[16]K. Kodama, Y. Yamashita, K. Toko, and T. Suemasu, Appl. Phys. Express **12**, 041005 (2019).

[17]R. Takabe, T. Deng, K. Kodama, Y. Yamashita, T. Sato, K. Toko, and T. Suemasu, J. Appl. Phys. **123**, 045703 (2018).

[18]Y. Yamashita, T. Sato, M. Emha Bayu, Kaoru Toko, T. Suemasu, Jpn. J. Appl. Phys. **57**, 075801 (2018).

[19]A. Uedono, T. Koida, A. Tsukazaki, M. Kawasaki, Z. Q. Chen, S. F. Chichibu, and H. Koinuma, J. Appl. Phys. **93**, 2481 (2003).

[20]A. Uedono, K. Shimodaira, M. Kiyohara, Z. Q. Chen, K. Yamabe, T. Ohdaira, R. Suzuki, and T. Mikado, J. Appl. Phys. **91**, 5307 (2002).

[21]R. Takabe, S. Yachi, W. Du, D. Tsukahara, H. Takeuchi, K. Toko, and T. Suemasu, AIP Advances **6**, 085107 (2016).

[22]R. Krause-Rehberg and H. S. Leipner, *Positron Annihilation in Semiconductors, Solid-State Sciences* (Springer-Verlag, Berlin, 1999) vol. 127.

[23]A. Uedono, I. Yonenaga, T. Watanabe, S. Kimura, N. Oshima, R. Suzuki, S. Ishibashi, and Y. Ohno, J. Appl. Phys. **114**, 084506 (2013).

[24]A. Uedono, T. Yamada, T. Hosoi, W. Egger, T. Koschine, C. Hugenschmidt, M. Dickmann, and H. Watanabe, Appl. Phys. Lett. **112**, 182103 (2018).

[25]R. Suzuki, T. Ohdaira, S. Ishibashi, A. Uedono, S. Niki, P. Fons, A. Yamada, T. Mikado, T. Yamazaki, and S. Tanigawa, Inst. Phys. Conf. Ser. **152**, 757 (1998).

[26]A. J. Nelson, A. M. Gabor, M. A. Contreras, R. Noufi, P. E. Sobol, P. Asoka-Kumar, and K. G. lynn, J. Appl. Phys. **78**, 269 (1995).

[27]R. Takabe, K. Nakamura, M. Baba, W. Du, M. A. Khan, K. Toko, M. Sasase, K. O. Hara, N. Usami, and T. Suemasu, Jpn. J. Appl. Phys. **53**, 04ER04 (2014).

[28]M. Somer, Z. Anorg. Allg. Chem. **626**, 2478 (2000).

[29]H. Peng, C. L. Wang, J. C. Li, R. Z. Zhang, M. X. Wang, Y. Sun, and M. Sheng, Phys. Lett. A **374**, 3797 (2010).

[30]K. O. Hara, N. Usami, Y. Hoshi, Y. Shiraki, M. Suzuno, K. Toko, and T. Suemasu, Jpn. J. Appl. Phys. **50**, 121202 (2011).

[31]T. Sato, H. Hoshida, R. Takabe, K. Toko, Y. Terai, and T. Suemasu, J. Appl. Phys. **124**, 025301 (2018).

[32]H. Hoshida, T. Suemasu, and Y. Terai, Defect and Diffusion Forum **386**, 43 (2018).

Fig. 1 (a) Photoresponse spectra of 0.5-μm-thick $BaSi_2$ grown at T_S = 580 °C with various R_{Ba}/R_{Si} measured under a bias voltage of −1.0 V applied to the front ITO electrode with respect to the back Al electrode.[17] (b) Dependences of the *S* parameter and carrier concentration on $BaSi_2$ films grown at T_S = 580 °C.

Fig. 2 (a) θ–2θ XRD and RHEED patterns of $BaSi_2$ films at T_S = 650 °C with various R_{Ba}/R_{Si} values. The asterisk (*) indicates the peak for the Si substrate used. (b) R_{Ba}/R_{Si} dependences of the FWHM of $BaSi_2$ 600 peak intensity for samples grown at T_S = 580 or 650 °C.

Fig. 3 Photoresponse spectra of 0.5-μm-thick $BaSi_2$ grown at T_S = 650 °C with various R_{Ba}/R_{Si} values measured under a bias voltage of –0.5 V applied to the front ITO electrode with respect to the back Al electrode. Broken line shows the photoresponse spectrum for the 580 °C with R_{Ba}/R_{Si} = 2.2.

Fig. 4 Raman spectra of samples grown at (a) 580 and (b) 650 °C with various values of R_{Ba}/R_{Si}. Arrows show the tiny peaks due to Si_{TO}. (c) R_{Ba}/R_{Si} dependences of the FWHM of Ag mode peak intensity at 490 cm^{-1} and the Si_{TO} peak intensity at 520 cm^{-1}.

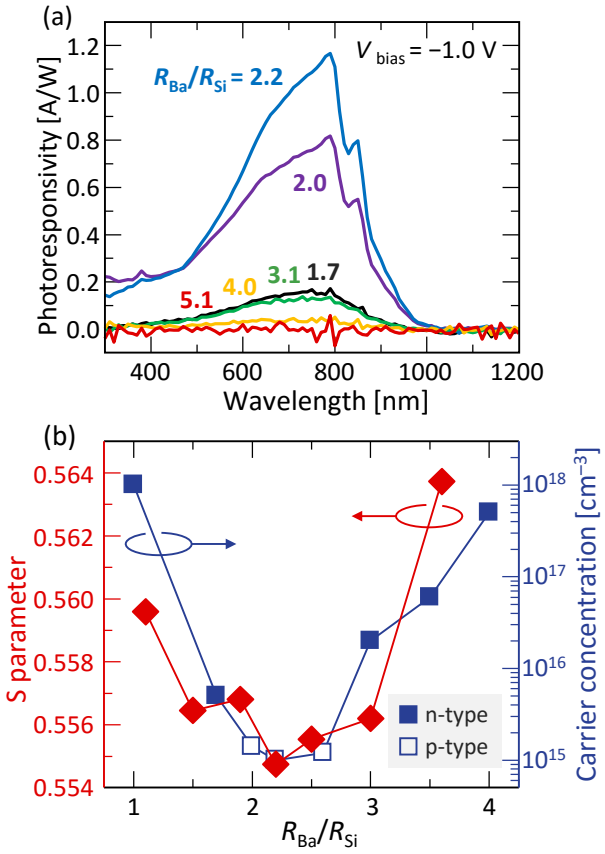
(a)
Photoresponsivity [A/W]
1.2
1.0
0.8
0.6
0.4
0.2
0.0
V_{bias} = −1.0 V
R_{Ba}/R_{Si} = 2.2
2.0
3.1
1.7
4.0
5.1
400
600
800
1000
1200
Wavelength [nm]
(b)
S parameter
0.564
0.562
0.560
0.558
0.556
0.554
Carrier concentration [cm^{-3}]
10^{18}
10^{17}
10^{16}
10^{15}
n-type
p-type
1
2
3
4
R_{Ba}/R_{Si}

Fig. 1

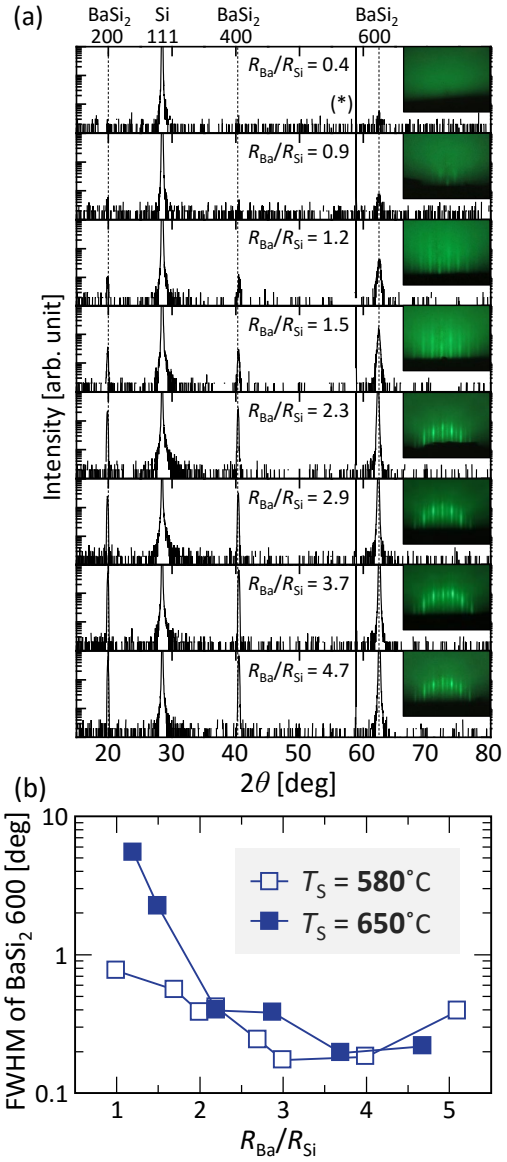
(a)
BaSi2 200
Si 111
BaSi2 400
BaSi2 600
RBa/RSi = 0.4
(*)
RBa/RSi = 0.9
RBa/RSi = 1.2
RBa/RSi = 1.5
RBa/RSi = 2.3
RBa/RSi = 2.9
RBa/RSi = 3.7
RBa/RSi = 4.7
Intensity [arb. unit]
20 30 40 50 60 70 80
2θ [deg]
(b)
FWHM of BaSi2 600 [deg]
10
1
0.1
TS = 580°C
TS = 650°C
1 2 3 4 5
RBa/RSi

Fig. 2

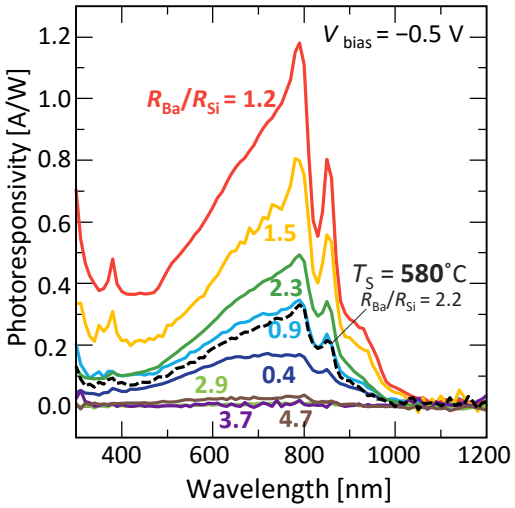
V_{bias} = −0.5 V
R_{Ba}/R_{Si} = 1.2
1.5
2.3
0.9
0.4
2.9
3.7
4.7
T_S = 580˚C
R_{Ba}/R_{Si} = 2.2
Photoresponsivity [A/W]
Wavelength [nm]
0.0
0.2
0.4
0.6
0.8
1.0
1.2
400
600
800
1000
1200

Fig. 3

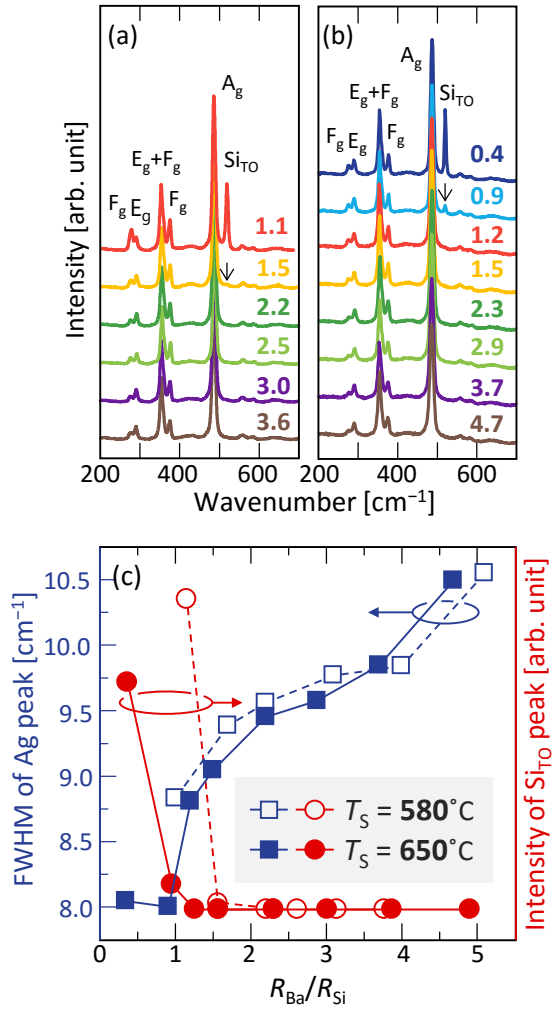
(a)
(b)
(c)
Intensity [arb. unit]
Wavenumber [cm⁻¹]
A_g
E_g+F_g
Si_TO
F_g E_g
F_g
1.1
1.5
2.2
2.5
3.0
3.6
0.4
0.9
1.2
1.5
2.3
2.9
3.7
4.7
FWHM of Ag peak [cm⁻¹]
Intensity of Si_TO peak [arb. unit]
R_Ba/R_Si
T_S = 580°C
T_S = 650°C

Fig. 4